

---

# FAST: a Fused and Accurate Shrinkage Tree for Heterogeneous Treatment Effects Estimation

---

Anonymous Author(s)  
Affiliation  
Address  
email

## Abstract

1 This paper proposes a novel strategy for estimating the heterogeneous treatment  
2 effect called the Fused and Accurate Shrinkage Tree (FAST). Our approach uti-  
3 lizes both trial and observational data to improve the accuracy and robustness of  
4 the estimator. Inspired by the concept of shrinkage estimation in statistics, we  
5 develop an optimal weighting scheme and a corresponding data-driven estimator  
6 that balances the unbiased estimator based on trial data with the potentially biased  
7 estimator based on observational data. Specifically, combining with tree-based  
8 techniques we introduce a new split criterion that utilizes both trial data and ob-  
9 servational data to more efficiently estimate treatment effect. Furthermore, we  
10 confirm the consistency of our proposed tree-based estimator and demonstrate the  
11 effectiveness of our criterion in reducing prediction error through theoretical anal-  
12 ysis. The advantageous finite sample performance of the FAST and its ensemble  
13 version over existing methods is demonstrated via simulations and real data anal-  
14 ysis.

## 15 1 Introduction

16 Causal effects are the magnitude of the response of an effect variable (also called outcome) caused  
17 by the effect variable (also called treatment), which is a fundamental and essential issue in the field  
18 of causal inference (Imbens and Rubin, 2016). And the heterogeneous treatment effect (abbr. HTE)  
19 is usually used to characterize the heterogeneity of causal effects across different subgroups of the  
20 population. In recent years, heterogeneous treatment effect estimation has been successfully applied  
21 in various fields such as epidemiology, medicine, and social sciences (Glass et al., 2013; Kosorok  
22 and Laber, 2019; Turney and Wildeman, 2015; Taddy et al., 2016).

23 In general, the causal problems can be studied through both experimental studies (also known as ran-  
24 domized control trials, RCTs) and observational studies. Experimental studies are widely regarded  
25 as the gold standard for assessing causal effects since the randomization process eliminates the pos-  
26 sibility of confounding bias. However, large-scale RCTs can be challenged due to issues related to  
27 cost, time, and ethics (Edwards et al., 1999). On the other hand, observational data are often readily  
28 available with an adequate sample size. Under certain fairly strong assumptions, such as uncon-  
29 foundedness assumption, there is a rich literature regarding the estimation of HTE in observational  
30 studies, such as tree-based methods (Athey and Imbens, 2016; Wager and Athey, 2018; Athey et al.,  
31 2019), boosting (Powers et al., 2017; Nie and Wager, 2020) and meta learners (Künzel et al., 2019;  
32 Nie and Wager, 2020). However, the unconfoundedness assumption, which requires measuring all  
33 confounders, is untestable and may lead to invalid causal inferences if violated. Various methods  
34 have been proposed to mitigate the unmeasured confounding in observational studies, such as the  
35 sensitivity analysis (Rosenbaum and Rubin, 1983; Zhang and Tchetgen Tchetgen, 2022), the instru-  
36 mental variables (IV) approach (Angrist et al., 1996) and the proximal causal inference (Kuroki and

37 Pearl, 2014; Miao et al., 2018; Shi et al., 2020; Cui et al., 2023). However, the validity of these  
 38 procedures also relies crucially on assumptions that are often difficult to verify in practice.

39 Given the limitations of relying on individual data sources, data fusion, as a branch of causal in-  
 40 ference strategies that integrates both the trial and the observational data, has gained significant  
 41 interest in the literature (Bareinboim and Pearl, 2016; Colnet et al., 2020; Shi et al., 2022). Existing  
 42 data fusion methods for estimating the HTE include the KPS estimator obtained by modeling the  
 43 confounding function parametrically (Kallus et al., 2018), the semi-parametric integrative estimator  
 44 under the parametric structural models (Yang et al., 2020) and the integrative R-learner (Wu and  
 45 Yang, 2022). Besides, (Tang et al., 2022) proposed the Gradient Boosting Causal Tree (GBCT),  
 46 which integrated the current observational data and their historical controls for estimating the condi-  
 47 tional average treatment effect on the treated group (CATT).

48 This paper presents a novel approach for estimating heterogeneous treatment effects (HTE) in the  
 49 context of causal data fusion. The proposed method, named Fused and Accurate Shrinkage Tree  
 50 (FAST), *avoids* the need for a two-stage estimation process required in conventional data fusion  
 51 strategies, which involves modeling and estimating the nuisance confounding bias function. The  
 52 main contributions of this work can be summarized as follows (i) The authors propose a novel  
 53 shrinkage method for combining an unbiased and biased estimator, which effectively reduces the  
 54 mean square error of the unbiased estimator, and provides an easy implementation of the method  
 55 tailored for the HTE estimation; (ii) They extend the conventional node split criterion via a re-scaling  
 56 technique, which automatically penalizes the use of the observational data with low quality (namely  
 57 large confounding bias); (iii) They also provide a theoretical analysis to explain the advantages of  
 58 our splitting criterion.

## 59 2 Background and motivation

### 60 2.1 Notations

61 Let  $\mathbf{X} \in \mathcal{X} = [-1, 1]^p$  be a  $p$ -dimensional vector of pre-treatment covariates,  $U \in \mathbb{R}^q$  be a possibly  
 62 unmeasured confounding variable,  $D$  be a binary treatment variable ( $D = 0$  denotes the control and  
 63  $D = 1$  denotes the treated) and let  $Y(d)$  be the potential outcome that would be observed when the  
 64 treatment had been set to  $d \in \{0, 1\}$ . We follow the potential outcome framework (Rubin, 1974) to  
 65 define the heterogeneous treatment effect  $\tau(\mathbf{x})$ , e.g.,  $\mathbb{E}(Y(1) - Y(0)|\mathbf{X} = \mathbf{x})$ .

66 Suppose that we can collect two kinds of data: trial data and observational data, and they are de-  
 67 scribed by  $n + m$  quadruples,  $\{Y_i, D_i, \mathbf{X}_i, S_i\}_{i=1}^{n+m}$ , where  $S_i$  indicates if the  $i$ -th individual would  
 68 have been recruited ( $S = 1$ ) or not ( $S = 0$ ) in the trial. We also denote  $\mathcal{R} = \{1, 2, \dots, n\}$  the set  
 69 of indices of observations in the RCT study, and  $\mathcal{O} = \{n + 1, n + 2, \dots, n + m\}$  the set of indices  
 70 of observations in the observational study. We define  $e(\mathbf{X}, \mathbf{U}, S) = P(D = 1|\mathbf{X}, \mathbf{U}, S)$  as the  
 71 propensity score of the trial and observational population, respectively. In practice, Due to  $\mathbf{U}$  being  
 72 unknown, we usually use  $\hat{e}(\mathbf{X}, S)$  to estimate  $e(\mathbf{X}, \mathbf{U}, S)$ . In addition,  $\hat{e}(\mathbf{X}, 1)$  is unbiased for the  
 73 randomization of trial data, but  $\hat{e}(\mathbf{X}, 0)$  is biased because the unmeasured confounder  $U$  is related  
 74 to the assignment of treatment  $D$ . Let  $\tau_1(\mathbf{x}) = \mathbb{E}(Y(1) - Y(0)|\mathbf{X} = \mathbf{x}, S = 1)$  be the HTE on the  
 75 trial population. We then make the following fundamental assumption on the trial and observational  
 76 studies, which facilitates the potential for causal data fusion:

77 **Assumption 1.** (i) For any  $\mathbf{x} \in \mathcal{X}$ ,  $\tau_1(\mathbf{x}) = \tau(\mathbf{x})$ ; (ii)  $Y(d) \perp D | (\mathbf{X}, S = 1)$  for  $d \in \{0, 1\}$  and  
 78 (iii) the propensity score  $0 < e(\mathbf{X}, S) < 1$  almost surely.

79 Assumption 1 (i) states that the HTE function is transportable from the trial population to the tar-  
 80 get population. Stronger versions of Assumption 1 include the ignorability of study participation  
 81 (Buchanan et al., 2018) and the mean exchangeability (Dahabreh et al., 2019). In the following of  
 82 this paper, we use  $|\Lambda|$  to denote the number of elements for any set  $\Lambda$ ,  $\lfloor c \rfloor$  to denote the biggest  
 83 integer less than or equal to the constant  $c$ , and  $[p]$  to denote the index set  $\{1, 2, \dots, \lfloor p \rfloor\}$ . For two  
 84 positive sequences  $\{a_n\}_{n \geq 1}$  and  $\{b_n\}_{n \geq 1}$ , we write  $a_n = O(b_n)$  if  $|a_n/b_n|$  is bounded.

### 85 2.2 Tree-based methods

86 To estimate the HTE, it is reasonable to perform subgroup analysis by appropriately stratifying or  
 87 matching (Frangakis and Rubin, 2002) the samples into multiple subgroups that differ in the magni-

88 tude of treatment effects. In machine learning, tree-based methods (Breiman et al., 1984; Breiman,  
 89 2001; Friedman, 2001) are usually used for such stratification tasks, which greedily optimize the  
 90 loss function, also called splitting criterion, via recursively partitioning feature space. In fact, many  
 91 tree-based causal methods designed for the HTE estimation were also proposed (Athey and Imbens,  
 92 2016; Athey et al., 2019; Radcliffe and Surry, 2012). For convenience, we define a regression tree  
 93 by two components: a set of leaves  $\mathbf{Q} = \{Q_j\}_{j=1}^J$  and the associated parameter  $\tau$ . We can denote  
 94 a causal tree by  $T(X; \mathbf{Q}, \tau) = \sum_{j=1}^J \tau(Q_j) \mathbb{I}\{\mathbf{x} \in Q_j\}$ , where  $\mathbb{I}\{\cdot\}$  denotes the indicator function  
 95 and  $\tau(Q_j)$  denotes the casual effect of sub-area indicated by  $Q_j$ .

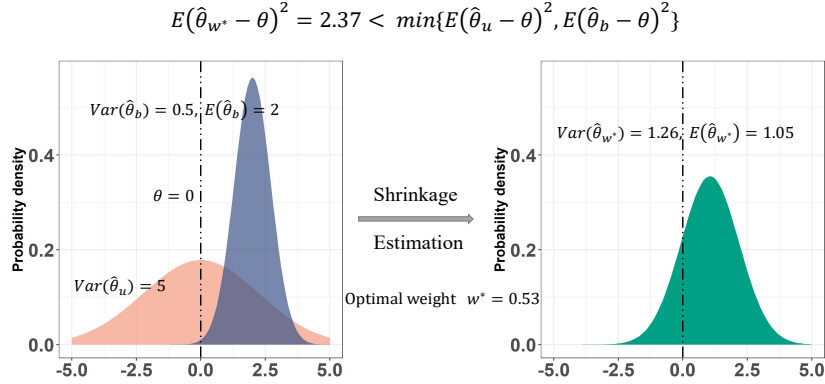


Figure 1: An illustration of the benefit of the shrinkage estimation strategy.

### 96 2.3 Shrinkage estimation

97 It is important to note that applying conventional methods, such as the generalized random forest  
 98 (Athey et al., 2019), separately to trial data and observational data can lead to two estimators: the first  
 99 is unbiased but may have high variance, while the second is potentially biased but has a smaller vari-  
 100 ance due to the larger amount of observational data. Therefore, the challenge becomes finding the  
 101 optimal combination of an unbiased estimator and a biased estimator in the data fusion problem. To  
 102 see this, suppose we have a parameter of interest  $\theta \in \mathbb{R}$ , an unbiased estimator  $\hat{\theta}_u$ , and a (potentially)  
 103 biased estimator  $\hat{\theta}_b$  of  $\theta$ , such that  $\mathbb{E}(\hat{\theta}_u) = \theta$ ,  $\mathbb{E}(\hat{\theta}_b) = \theta + b(\theta)$ ,  $\text{Var}(\hat{\theta}_u) = \sigma_u^2$ ,  $\text{Var}(\hat{\theta}_b) = \sigma_b^2$  and  
 104  $\text{Cov}(\hat{\theta}_u, \hat{\theta}_b) = 0$ . Consider the family of estimators  $\Lambda_w = \{\hat{\theta}_w | \hat{\theta}_w = w\hat{\theta}_b + (1-w)\hat{\theta}_u, 0 \leq w \leq 1\}$ ,  
 105 then the mean square error (MSE) of its elements admits the following expansion:

$$\mathbb{E}(\hat{\theta}_w - \theta)^2 = (\sigma_b^2 + b^2(\theta) + \sigma_u^2)w^2 - 2\sigma_u^2w + \sigma_u^2. \quad (1)$$

106 Minimizing (1) with respect to  $w$ , we can obtain the unique minimizer  $w^* = \sigma_u^2 / (\sigma_b^2 + b^2(\theta) + \sigma_u^2)$   
 107 and the gain of the optimal weighting can be characterized by the following formula

$$\mathbb{E}(\hat{\theta}_{w^*} - \theta)^2 = (1 - w^*)\sigma_u^2 = w^*(\sigma_b^2 + b^2(\theta)). \quad (2)$$

108 **Comment** The weighting strategy is akin to the classical James-Stein shrinkage estimation (Efron  
 109 and Morris, 1973; Green and Strawderman, 1991) method, in which it is shown that a multivariate  
 110 normal vector  $\mathbf{Z}$  ( $p \geq 3$ ), as a maximum likelihood estimator (MLE) of its population mean  $\boldsymbol{\mu} =$   
 111  $\mathbb{E}(\mathbf{Z})$ , is not minimax, and the MSE of the estimator  $\mathbf{Z}$  can be reduced by shrinking it towards the  
 112 zero vector  $\mathbf{0}$  by some factor  $0 < w < 1$ . The zero vector can be viewed as a biased estimator of  
 113  $\boldsymbol{\mu}$  with zero variance in their setting. In comparison, we replace the deterministic estimator with a  
 114 (potentially) biased estimator  $\hat{\theta}_b$ : The larger the variance  $\sigma_u^2$  of the unbiased estimator is compared to  
 115  $b^2(\theta) + \sigma_b^2$ , the more the fused estimator  $\hat{\theta}_{w^*}$  will be shrunk towards the biased estimator that is less  
 116 fluctuating. By doing so, one can efficiently mitigate the occurrence of significant estimation error  
 117 in the unbiased estimator caused by its high variance, as unbiasedness alone *does not* guarantee  
 118 reliable estimation performance in a finite sample. Figure 1 illustrates a concrete example of the

119 benefit provided by the shrinkage estimation, where  $\theta = 0$ ,  $\hat{\theta}_u \sim N(\theta, 5)$  and  $\hat{\theta}_b \sim N(\theta + 2, 0.5)$ .  
 120 The fused estimator  $\hat{\theta}_{u^*}$  reduces over 50% of the MSE compared with the unbiased estimator  $\hat{\theta}_u$ .

### 121 3 Methodology

122 In this section, we propose a new data fusion strategy, referred to as the Fused and Accurate Shrinkage  
 123 Tree (FAST). We proceed in a bottom-up manner to provide a clear and intuitive illustration of  
 124 the entire estimation: we will begin by applying the shrinkage estimation strategy for local data fusion  
 125 within each sub-region of the feature space given by a pre-specified partition. Then, we propose  
 126 a fused criterion that incorporates the information contained in the observational data via a simple  
 127 re-scaling of the conventional criterion. Theoretical guarantees are established in Section 4.

#### 128 3.1 Local fusion for the HTE estimation

129 Under a pre-specified partition  $\mathbf{Q} = \{Q_j\}_{j=1}^J$  of the feature space, let  $\mathcal{R}_j = \{i | i \in \mathcal{R}, \mathbf{X}_i \in Q_j\}$   
 130 and  $\mathcal{O}_j = \{i | i \in \mathcal{O}, \mathbf{X}_i \in Q_j\}$  represent the sets of indices of the trial and observational sub-  
 131 samples, respectively, that fall within the region  $Q_j$ . Let

$$\tilde{Y} = \frac{YD}{e(\mathbf{X}, S)} - \frac{Y(1-D)}{1-e(\mathbf{X}, S)} \quad (3)$$

132 be transformed outcomes of all data, e.g., the transformed outcomes of  $i$ -th sample can be denoted  
 133 by  $\tilde{Y}_i$ . Then under Assumption 1, one is able to verify that

$$\mathbb{E}(\tilde{Y} | \mathbf{X} = \mathbf{x}, S = 1) = \tau_1(\mathbf{x}) = \tau(\mathbf{x}). \quad (4)$$

134 Thus,  $\hat{\tau}_u(Q_j) = (1/|\mathcal{R}_j|) \sum_{i \in \mathcal{R}_j} \tilde{Y}_i$  is an unbiased estimator of  $\mathbb{E}(Y(1) - Y(0) | \mathbf{X} \in Q_j, S = 1)$ ,  
 135 which can be seen as a reasonable approximation of  $\tau(Q_j)$  if  $\mathbf{Q}$  segments the feature space properly  
 136 such that  $\tau(\mathbf{x})$  varies slowly in each sub-region  $Q_j$ . An estimator of  $\text{Var}(\hat{\tau}_u(Q_j))$  is given by  
 137  $\hat{\sigma}_u^2(Q_j) = (1/(|\mathcal{R}_j|(|\mathcal{R}_j| - 1))) \sum_{i \in \mathcal{R}_j} (\tilde{Y}_i - \hat{\tau}_u(Q_j))^2$ . In contrast,  $\hat{\tau}_b(Q_j) = (1/|\mathcal{O}_j|) \sum_{i \in \mathcal{O}_j} \tilde{Y}_i$   
 138 is a biased estimator concerning  $\tau(Q_j)$ , due to the presence of unmeasured confounding ( $U$ ) on the  
 139 observational data.

140 It remains to estimate the region-specific weight  $w^*(Q_j)$ , amounting to the estimation of the tuple  
 141  $(\sigma_u^2(Q_j), \sigma_b^2(Q_j), b^2(Q_j))$ . The first term  $\sigma_u^2(Q_j)$  can be estimated by  $\hat{\sigma}_u^2(Q_j)$ . To bypass the  
 142 unmeasured confounding issue of the observational population, re-sampling techniques, such as the  
 143 Bootstrap (Efron, 1979; Hall, 1992), can be applied to estimate  $\sigma_b^2(Q_j)$ . Alternatively,  $\sigma_b^2(Q_j) =$   
 144  $O(|\mathcal{O}_j|^{-1})$  is expected to be of a smaller order term compared to  $\sigma_u^2(Q_j) = O(|\mathcal{R}_j|^{-1})$  in practice,  
 145 which is a consequence of the relative sample size between the trial and the observational data. Thus,  
 146 one can avoid estimating the negligible term  $\sigma_b^2(Q_j)$ . For the last term,  $\widehat{b(Q_j)} = \hat{\tau}_b(Q_j) - \hat{\tau}_u(Q_j)$   
 147 serves as a natural estimator of the bias  $b(Q_j)$ . This leads to the following estimator of  $w^*(Q_j)$  and  
 148 the corresponding fused estimator

$$\hat{w}_{of}(Q_j) = \hat{\sigma}_u^2(Q_j) / (\hat{\sigma}_u^2(Q_j) + (\widehat{b(Q_j)})^2) \quad \text{and} \quad (5)$$

$$\hat{\tau}_{of}(Q_j) = \hat{w}_{of}(Q_j) \hat{\tau}_b(Q_j) + (1 - \hat{w}_{of}(Q_j)) \hat{\tau}_u(Q_j). \quad (6)$$

150 A fused estimator of the HTE function  $\tau(\cdot)$  under the partition  $\mathbf{Q}$  can thus be defined as  $\hat{\tau}_{\mathbf{Q}}(\mathbf{x}) =$   
 151  $\sum_{j=1}^J \hat{\tau}_{of}(Q_j) \mathbb{I}\{\mathbf{x} \in Q_j\}$ .

#### 152 3.2 Adaptive fusion for segmentation

153 In order to obtain a tree-based partition  $\mathbf{Q}$  designed for the fusion strategy (6), a split criterion  
 154 is required, which is sufficient to be defined only at the root node given the recursive nature of  
 155 the partitioning. We follow the honest estimation approach (Athey and Imbens, 2016) to prevent  
 156 overfitting. Specifically, given a fraction  $0 < r < 1$  (typically  $r = 0.5$ ),  $\lfloor rn \rfloor$  observations are  
 157 sampled without replacement from the trial data of sample size  $n$  for the tree structure estimation,  
 158 while the rest of observations are used for local estimation of the HTE in each leaf node. Let the  
 159 index sets of the trial data used for the partition and the HTE estimation be  $\mathcal{R}^t$  and  $\mathcal{R}^e$ , respectively.

160 We do not further split the observational data to reduce uncertainty, since we have already partitioned  
 161 the trial data to avoid overfitting.

162 The conventional criterion for growing a regression tree chooses the index of the split variable and  
 163 its split value at the root node by minimizing the following goodness-of-fit criterion

$$(\hat{q}, \hat{c}) = \arg \min_{\hat{q} \in [p], \hat{c} \in \mathbb{R}} \left( \sum_{i \in \hat{\mathcal{R}}_L^t} \left( \tilde{Y}_i - \hat{\tau}_u(\hat{Q}_L, \mathcal{R}^t) \right)^2 + \sum_{i \in \hat{\mathcal{R}}_R^t} \left( \tilde{Y}_i - \hat{\tau}_u(\hat{Q}_R, \mathcal{R}^t) \right)^2 \right), \quad (7)$$

164 where  $\hat{Q}_L = \{\mathbf{x} | \mathbf{x}_{\hat{q}} \leq \hat{c}\}$ ,  $\hat{\mathcal{R}}_L^t = \{i | i \in \mathcal{R}^t, \mathbf{X}_i \in \hat{Q}_L\}$  and  $\hat{\tau}_u(\hat{Q}_L, \mathcal{R}^t) = (1/|\{i | i \in \mathcal{R}^t, \mathbf{X}_i \in$   
 165  $\hat{Q}_L\}|) \sum_{i \in \{i | i \in \mathcal{R}^t, \mathbf{X}_i \in \hat{Q}_L\}} \tilde{Y}_i$ , and  $\hat{Q}_R$ ,  $\hat{\mathcal{R}}_R^t$  and  $\hat{\tau}_u(\hat{Q}_R, \mathcal{R}^t)$  can be defined correspondingly.  
 166 Given a tree grown under (7), we fuse the trial data indexed by  $\mathcal{R}^e$  and the observational data  
 167 indexed by  $\mathcal{O}$  at each leaf node according to (6) and refer to the resulting tree estimator as a **Shrink-**  
 168 **age Tree** (ST). A direct modification of (7), which aligns more with the fused estimator at the leaf  
 169 nodes, should be

$$(\hat{q}, \hat{c}) = \arg \min_{\hat{q} \in [p], \hat{c} \in \mathbb{R}} \left( \sum_{i \in \hat{\mathcal{R}}_L^t} \left( \tilde{Y}_i - \hat{\tau}_{of}(\hat{Q}_L) \right)^2 + \sum_{i \in \hat{\mathcal{R}}_R^t} \left( \tilde{Y}_i - \hat{\tau}_{of}(\hat{Q}_R) \right)^2 \right), \quad (8)$$

170 where  $\hat{\tau}_{of}(\hat{Q}_L) = \hat{w}_{of}(\hat{Q}_L) \hat{\tau}_b(\hat{Q}_L) + (1 - \hat{w}_{of}(\hat{Q}_L)) \hat{\tau}_u(\hat{Q}_L, \mathcal{R}^t)$  and  $\hat{\tau}_{of}(\hat{Q}_R)$  is defined corre-  
 171 spondingly. The replacement of the unbiased estimators in (7) with the fused estimators in (8)  
 172 facilitates a goodness-of-fit criterion of the proposed fusion strategy.

173 Alternatively, (7) can be interpreted as minimizing the sum of the estimated MSEs of the unbiased  
 174 estimators at the child nodes, if the two terms on the right-hand side of (7) are divided by the square  
 175 of their respective sample sizes. By contrast, since the fused estimator  $\hat{\tau}_{of}$  reduces variance by  
 176 shrinking the original unbiased estimator to a potentially biased estimator, simply comparing the  
 177 fused estimators with the outcomes of the trial data as in (8) fails to capture the variability at the  
 178 child nodes. Instead, an appropriate criterion shall respect the MSE of the fused estimator. To this  
 179 end, we introduce the following split criterion

$$(\hat{q}, \hat{c}) = \arg \min_{\hat{q} \in [p], \hat{c} \in \mathbb{R}} \left( (1 - \hat{w}_{of}(\hat{Q}_L)) \hat{\sigma}_u^2(\hat{Q}_L, \mathcal{R}^t) + (1 - \hat{w}_{of}(\hat{Q}_R)) \hat{\sigma}_u^2(\hat{Q}_R, \mathcal{R}^t) \right), \quad (9)$$

180 where  $(1 - \hat{w}_{of}(\hat{Q}_L)) \hat{\sigma}_u^2(\hat{Q}_L, \mathcal{R}^t)$  and  $(1 - \hat{w}_{of}(\hat{Q}_R)) \hat{\sigma}_u^2(\hat{Q}_R, \mathcal{R}^t)$  estimate the MSE of  $\hat{\tau}_{of}(\hat{Q}_L)$   
 181 and  $\hat{\tau}_{of}(\hat{Q}_R)$ , respectively, according to formula (2). Compared to (7), the proposed criterion incor-  
 182 porates the additional information from the observational data into each node split in an adaptive  
 183 manner by simply re-scaling the estimated MSE of the unbiased estimator.

184 **Comment** The criterion (9) offers the benefit of local adjustment, which can be intuitively justified.  
 185 In sub-regions where the observational data exhibit moderate confounding biases, this criterion im-  
 186 proves tree building by providing a sharper assessment of the variability of the fused estimator. On  
 187 the other hand, for sub-regions where the observational data exhibit substantial confounding biases,  
 188 the estimated weights of those sub-regions approach zero according to (5). In such cases, the cri-  
 189 terion reduces to the conventional criterion (7), except for the standardization of the square of the  
 190 sample size. It is worth mentioning that all the local adjustments achieved by applying this adaptive  
 191 fusion strategy are data-driven, namely one can just avoid global modeling of the confounding bias  
 192 function, which requires domain-specific knowledge of the observational studies. Additionally, it  
 193 also enables the exclusion of the global impact of extremely large confounding biases of the obser-  
 194 vational data that only exist in certain sub-regions of the feature space.

195 We denote the partition obtained under criterion (9) as  $\hat{Q}_{of} = \{\hat{Q}_{of,1}, \hat{Q}_{of,2}, \dots, \hat{Q}_{of,|\hat{Q}_{of}|}\}$ , and  
 196 the corresponding tree-based estimator of the HTE is defined as

$$\hat{\tau}_{fast}(\mathbf{x}) = \sum_{j=1}^{|\hat{Q}_{of}|} \hat{\tau}_{of}^e(\hat{Q}_{of,j}) I\{\mathbf{x} \in \hat{Q}_{of,j}\}, \quad (10)$$

197 where the superscript “e” is to show that the RCT data used to construct the fused estimator at the leaf  
 198 node is indexed by  $\mathcal{R}^e$  and “fast” is an acronym for the name Fused and Accurate Shrinkage Tree,  
 199 which is due to the data fusion nature of the criterion (9), the shrinkage-type leaf node estimator (6)  
 200 and its accuracy in terms of the MSE.

201 **3.3 Ensemble fusion**

202 To reduce overfitting, improve robustness against outliers, and enhance generalization, we introduce  
 203 the bagged version (Hastie et al., 2009) of the FAST, referred to as the rfFAST, as follows: We  
 204 randomly draw index sets  $\mathcal{R}^*$  of size  $n$  and  $\mathcal{O}^*$  of size  $m$ , separately from  $\mathcal{R}$  and  $\mathcal{O}$  with replacement.  
 205 We repeat the process  $B$  times, resulting in  $\{\mathcal{R}^{*,(b)}, \mathcal{O}^{*,(b)}\}_{b=1}^B$ . Then,  $B$  estimators  $\hat{\tau}_{fast}^{*,(b)}(\mathbf{x})$  can be  
 206 calculated based on the trial data indexed by  $\mathcal{R}^{*,(b)}$  and the observational data index by  $\mathcal{O}^{*,(b)}$ . We  
 207 then define  $\hat{\tau}_{rfast}(\mathbf{x}) = (1/B) \sum_{b=1}^B \hat{\tau}_{fast}^{*,(b)}(\mathbf{x})$ . A detailed algorithm is given in the supplementary  
 208 material and for the construction of the prediction intervals, see Zhang et al. (2020).

209 **4 Theoretical guarantee**

210 In this section, we formally establish the benefits of the proposed split criterion (9) compared with  
 211 the conventional criterion (7). To present the theoretical result, we first pose the following regularity  
 212 conditions that are standard in literature (see e.g., Györfi et al., 2002 and Scornet et al., 2015).

213 **Assumption 2.** (i) *There exists a positive constant  $\lambda < \infty$  such that  $\mathbb{E}\{\exp(\lambda \tilde{Y}^2) | S = i\} < \infty$  for*  
 214  *$i = 0, 1$ .* (ii) *There exists positive constants  $\sigma_{\min} < \infty$  such that  $\sigma_{\min}^2 < \text{Var}(\tilde{Y} | \mathbf{X} = \mathbf{x}, S = 0)$*   
 215 *for any  $\mathbf{x} \in \mathcal{X}$ .*

216 **Theorem 1** (MSE reduction of the proposed split criterion). *Let  $\theta = (q, c)$  and  $\Theta = [p] \times \mathbb{R}$ .*  
 217 *Suppose the node that needs to be partitioned is  $Q_j$ , under which the sample sizes of the trial data*  
 218 *and observational data are  $n_j$  and  $m_j$ , respectively. Let  $M(\theta)$  and  $M_{of}(\theta)$  be the sum of MSEs of*  
 219 *the conventional HTE estimator and the fused HTE estimator on the two child nodes of  $Q_j$  split by  $\theta$ ,*  
 220 *respectively. Denote  $b_{\min} = \inf_{\mathbf{x} \in Q_j} \{\mathbb{E}(\tilde{Y} | \mathbf{X} = \mathbf{x}, S = 0) - \mathbb{E}(\tilde{Y} | \mathbf{X} = \mathbf{x}, S = 1)\}$ . Let  $\hat{\theta}$  be the*  
 221 *solution of the conventional split criterion (7) and  $\hat{\theta}_{of}$  be the solution of the proposed split criterion*  
 222 *(9). Under Assumptions 1-2, we have*

223 (i) *For any  $\theta \in \Theta$ ,*

$$\frac{M_{of}(\theta)}{M(\theta)} - 1 \leq -\frac{\sigma_{\min}^2}{\sigma_{\min}^2 + n_j b_{\min}^2}. \quad (11)$$

224 (ii) *With probability at least  $1 - C_1 e^{-t}$  for some positive constant  $C_1 < \infty$ , it holds that*

$$M(\hat{\theta}) - M(\theta^*) \leq C_2 \frac{t + \log(pn_j) \log^4(n_j)}{n_j}, \quad (12)$$

$$\text{and } M_{of}(\hat{\theta}_{of}) - M_{of}(\theta_{of}^*) \leq C_3 \left( \frac{t + \log(pn_j) \log^4(n_j)}{m_j} + \frac{t + \log(pn_j) \log^4(n_j)}{n_j} \right), \quad (13)$$

225 *for some positive constant  $C_2, C_3 < \infty$ , where  $\theta^*$  and  $\theta_{of}^*$  are oracle splits defined as*

$$\theta^* = \arg \min_{\theta \in \Theta} M(\theta) \quad \text{and} \quad \theta_{of}^* = \arg \min_{\theta \in \Theta} M_{of}(\theta).$$

226 In the above theorem, the (i) part establishes a uniform MSE reduction result for any split choice  
 227  $\theta \in \Theta$  of the proposed split criterion (9). As revealed in (11), the criterion (9) leads to larger  
 228 MSE reduction on the nodes with a larger variance of  $\tilde{Y}$  and less bias of the observational data. In  
 229 addition, the upper bound in (11) decreases as the node sample size  $n_j$  decreases, implying that  
 230 our proposed criterion leads to increasing relative benefits as the tree grows deeper. Besides, in  
 231 the (ii) part we present non-asymptotic bounds for the discrepancies between the MSEs under the  
 232 empirically estimated splits and the oracle splits, showing that the MSEs under the estimated splits  
 233 can achieve a fast convergence rate. As a direct consequence of Theorem 1, the consistency of our  
 234 final HTE estimator (10) can be established, since it is known from Scornet et al. (2015) and Athey  
 235 et al. (2019) that the conventional tree-based estimator using only the trial data is mean-squared  
 236 consistent, and our proposed method leads to a reduced MSE.

237 **Proposition 1** (Consistency of  $\hat{\tau}_{fast}$ ). *For almost every  $\mathbf{x} \in [-1, 1]^p$ , we have  $\hat{\tau}_{fast}(\mathbf{x}) \rightarrow \tau(\mathbf{x})$  in*  
 238 *probability as  $n, m \rightarrow \infty$ .*

## 239 5 Experiments

240 In this section, we will demonstrate the results of a series of experiments to answer the following two  
241 questions: (i) Whether the proposed method can effectively alleviate the impact of confounding bias  
242 of observational data and limited sample size of trial data; (ii) Whether the techniques we proposed  
243 including local fusion in tree leaves and adaptive fusion in partitioning are valid, respectively.

244 In consequence, we conducted experiments on both simulated and real-world datasets to verify the  
245 effectiveness of our method. We evaluated our method against both traditional tree-based and data  
246 fusion-based casual methods. The former includes the classical Transformed Outcome Honest Tree  
247 (HT) Athey and Imbens (2016) and its ensemble version Generalized Random Forest (GRF) Athey  
248 et al. (2019). The latter includes the simplest fusion estimator (SF) training both trial data and  
249 observational data together without distinction and the KPS estimators Kallus et al. (2018). In order  
250 to facilitate better comparison and understanding of our proposed method, we demonstrate three  
251 versions: the simple implementation, Shrinkage Tree (ST), described in Section 3.1; the improved  
252 version, Fused and Accurate Shrinkage Tree (FAST), described in Section 3.2; and its final ensemble  
253 version rfFAST described in Section 3.3. The results of each simulation experiment were based on  
254  $B = 100$  replications. The ensemble size for all the ensemble estimators was set to 100. For the  
255 tree estimators, the minimum number of observations required to be at a leaf node was set to 5 and  
256 the maximum depth of the tree was set to 10.

### 257 5.1 Simulation

258 We conducted two sets of simulation experiments to evaluate the finite sample performance of the  
259 fused estimator and various baseline estimators. In both experiments, we first generated the pre-  
260 treatment covariates  $\mathbf{X} = (X_1, X_2, \dots, X_p)^T$  from  $\text{Uniform}[-1, 1]^p$  and the unobserved variable  
261  $U$  from  $\text{N}(0, 1)$ . Then, we generated the potential outcomes by  $Y(d) = d\tau(\mathbf{X}) + \sum_{j=1}^p X_j + 1.5U +$   
262  $\epsilon(d)$ , where  $\tau(\mathbf{X}) = 1 + X_1 + X_1^2 + X_2 + X_2^2$  and  $\epsilon(d) \sim \text{N}(0, 1)$  for  $d = 0, 1$ . Thus The treatment  
263 assignments for the trial sample of size  $n$  and the observational sample of size  $m$  were generated as  
264 follows:  $D|(\mathbf{X}, U, S = 1) \sim \text{Ber}(0.5)$  and  $D|(\mathbf{X}, U, S = 0) \sim \text{Ber}(1/(1 + \exp(-\beta U - 0.5X_1)))$ .  
265 Thus, the magnitude of  $\beta$  controls the strength of the unmeasured confounding: a larger  $\beta$  leads to a  
266 larger confounding bias. The test data  $X_{test,j}$  for  $1 \leq j \leq p$  were generated from  $\text{Uniform}(-1, 1)$   
267 with sample size 1000.

268 In the first experiment, we aim to verify the effectiveness of the proposed data fusion strategy via  
269 an ablation study. We compared the robustness of the ST and the FAST against different levels  
270 of confounding bias parameter  $\beta$ . Two baselines were considered: (i) the HT using only the trial  
271 data and (ii) the SF estimator obtained by directly merging all the available data and constructing a  
272 Fit-Based Causal Tree (Athey and Imbens, 2016). We set the sample sizes of the trial data and the  
273 observational data be  $n = 200$  and  $m = 2000$ , respectively, the dimension of covariates  $p = 5$  and  
274  $\beta \in \{0.1c | c \in \mathbb{N}, c \leq 19\}$ . The following three conclusions can be drawn from Figure 2: (1) When  
275 confounding bias in observational data was small, the simple fusion (SF) strategy can effectively im-  
276 prove the model performance. But when it became large, the SF was very vulnerable to confounding  
277 bias in observational data; (2) Even with the increase of  $\beta$ , both ST and FAST consistently showed  
278 resistance to confounding bias; (3) FAST was significantly better than other methods including ST,  
279 which verified the effectiveness of our proposed split criterion (9) numerically.

280 In the second experiment, we evaluated the RMSEs with respect to different  $n$  and  $\beta$ . We set  
281  $m = 2000$  and  $p = 5$ . We included seven estimators in the analysis: The first two estimators  
282 were calculated purely based on the trial data: (i) the Transformed Outcome Honest Tree (HT)  
283 (Athey and Imbens, 2016) and (ii) the Generalized Random Forest (GRF) (Athey et al., 2019).  
284 The rest estimators were calculated using different data fusion strategies: (iii) the Shrinkage Tree  
285 (ST) estimator, (iv) the Fused and Accurate Shrinkage Tree (FAST) estimator, (v& vi) the KPS  
286 estimators (Kallus et al., 2018) with a parametric (OLS) estimator and a non-parametric (Random  
287 Forest) specification of the confounding function, respectively and (vii) the bagged FAST estimator  
288 (rfFAST).

289 Table 1 reports the RMSEs of the seven estimators, conveying a good estimation accuracy of both  
290 the FAST and its ensemble version rfFAST. Among the three individual estimators, the ST and  
291 FAST, exhibited superior performance compared to the HT, and the FAST outperformed the ST.  
292 These relative performances provided support for the FAST approach compared to the classical

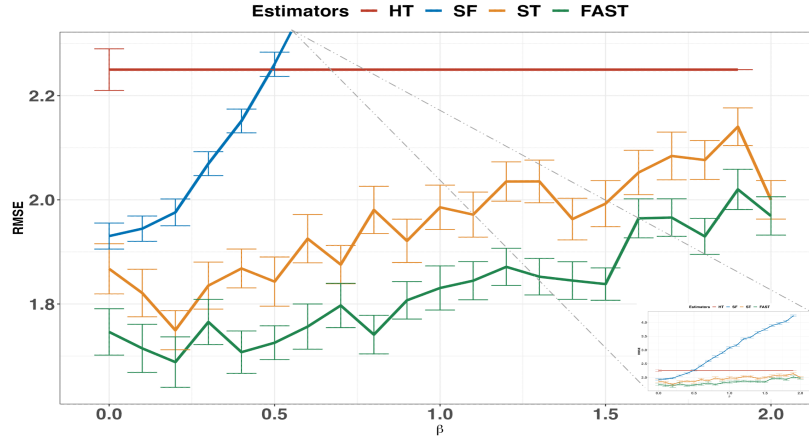


Figure 2: The averaged root mean square error (RMSE) (mean with  $2 \times$  s.d. error bars) of each algorithm on multiple simulation datasets with different levels of the confounding bias parameter  $\beta$ .

Table 1: The averaged RMSE (standard error in parentheses) of the estimators with respect to the trial sample size  $n$  and the confounding bias parameter  $\beta$ . The best performance is marked in **bold**.

$n$	$\beta$	HT	ST	FAST	GRF	$KPS_{ols}$	$KPS_{RF}$	rfFAST
100	0.5		1.89 (0.06)	1.84 (0.06)		1.33 (0.04)	1.73 (0.03)	<b>0.84</b> (0.02)
	1.0	2.28 (0.06)	1.90 (0.05)	1.85 (0.05)	1.12 (0.02)	1.29 (0.04)	1.65 (0.03)	<b>0.89</b> (0.02)
	2.0		2.05 (0.05)	2.02 (0.04)		1.28 (0.04)	1.71 (0.03)	<b>0.98</b> (0.02)
200	0.5		1.87 (0.04)	1.71 (0.04)		0.96 (0.02)	1.56 (0.02)	<b>0.73</b> (0.01)
	1.0	2.20 (0.04)	1.98 (0.04)	1.83 (0.04)	1.19 (0.01)	0.97 (0.03)	1.59 (0.02)	<b>0.84</b> (0.02)
	2.0		2.08 (0.03)	1.97 (0.03)		1.01 (0.02)	1.57 (0.03)	<b>0.92</b> (0.02)

293 honest regression tree, the proposed split criterion (9), and the shrinkage estimation strategy (6),  
 294 which are implemented progressively. Among the three ensemble estimators, the rfFAST estimator  
 295 demonstrated the best performance among all the six combinations of the trial sample size  $n$  and the  
 296 confounding bias parameter  $\beta$ . On the other hand, the performance of the KPS estimators appeared  
 297 to be less stable. The  $KPS_{ols}$  outperformed the GRF only when the trial sample size was relatively  
 298 large ( $n = 200$ ). Under the non-parametric specification of the confounding function, the  $KPS_{RF}$   
 299 did not gain benefit from incorporating the observational data and was consistently inferior to the  
 300 baseline estimator GRF.

## 301 5.2 Real-world data

302 In this sub-section, we report an analysis of the Tennessee Student/Teacher Achievement Ratio  
 303 (STAR) Experiment (Krueger, 1999) to demonstrate the proposed FAST for the HTE estimation.  
 304 We aim at quantifying the treatment effect of the class size on the student’s academic achievement.

305 **Data description** The STAR Experiment was a randomized controlled trial conducted in the late  
 306 1980s. Students were randomly assigned to one of the two types of classes during the first school  
 307 year:  $D = 1$  for small classes containing 13 – 17 pupils and  $D = 0$  for regular classes containing  
 308 22 – 25 pupils. The outcome  $Y$  is the average of the listening, reading, and math standardized tests  
 309 at the end of first grade. The vector of covariates  $X$  includes gender, race, birth month, birthday,  
 310 birth year, free lunch given or not, and teacher id. This made a universal sample of 4218 students,

311 among which 2413 were randomly assigned to regular-size classes ( $D = 0$ ) and 1805 to small  
 312 classes ( $D = 1$ ).

313 **Ground-truth** In practice, the ground-truth  $\tau(\cdot)$  is not accessible, so we replaced it with an estimate  
 314 calculated by a generalized random forest (Athey et al., 2019) based on all the 4218 observations.

315 **Construction of the trial, observational and test data** Following Kallus et al. (2018), we intro-  
 316 duced confounding bias by splitting the population over a variable which is known to strongly affect  
 317 the observed outcome  $Y$  (Krueger, 1999): rural or inner-city ( $U = 1$ , 2811 students) and urban or  
 318 suburban ( $U = 0$ , 1407 students). The trial data were generated by randomly sampling a fraction  $h$   
 319 of the students with  $U = 1$ , where  $h$  ranges from 0.1 to 0.5. The observational data were constructed  
 320 as follows: From students with  $U = 1$ , we took the controls ( $D = 0$ ) that were not sampled in trial  
 321 data, and the treated ( $D = 1$ ) whose outcomes were in the lower half of outcomes among students  
 322 with  $D = 1$  and  $U = 1$ ; From students with  $U = 0$ , we took all of the controls ( $D = 0$ ), and the  
 323 treated ( $D = 1$ ) whose outcomes were in the lower half of outcomes among students with  $D = 1$   
 324 and  $U = 0$ . The test data consisted of a held-out sub-sample of all the observations in the universal  
 325 sample excluding the trial data. For detailed pre-processing of the data, see the supplementary file.

326 **Results** We compared the performance of the rfFAST with various baseline estimators. In partic-  
 327 ular, the NF and the SF estimators were constructed using the Random Forest regressor. The NF  
 328 estimator utilized only trial data, while the SF estimator utilized both trial data and observational  
 329 data together without distinction. As shown in Figure 3, the proposed rfFAST method consistently  
 outperformed other estimators.

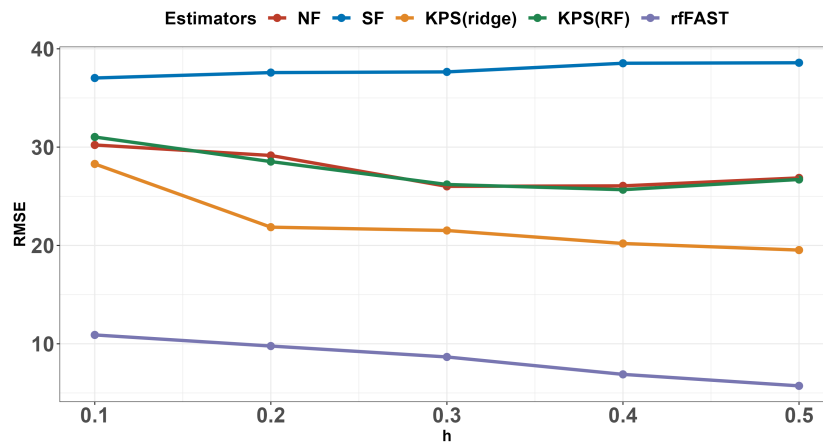


Figure 3: The RMSEs of the five estimators with respect to different sample sizes of the trial data, reflected by the fraction parameter  $h$ . A large  $h$  means a large trial sample size.

330

## 331 6 Discussion

332 This paper explores the estimation of heterogeneous treatment effects (HTE) within the framework  
 333 of causal data fusion. Drawing inspiration from the classical James-Stein shrinkage estimation  
 334 (Green and Strawderman, 1991) approach, the authors introduce a new method called Fused and  
 335 Accurate Shrinkage Tree (FAST) that effectively incorporates observational data in both feature  
 336 space segmentation and leaf node value estimation. This new approach is shown to outperform  
 337 existing data fusion methods via numerical experiments.

338 The above estimation framework can be generalized to any data fusion problem if there exists an  
 339 unbiased estimator and a biased estimator of some functions of interest. It would be worthwhile to  
 340 explore the combination of the FAST method with other ensemble methods, such as the boosting  
 341 and the grf-style (Athey et al., 2019) bagging, in addition to Breiman-style (Breiman, 2001) bagging  
 342 used in rfFAST. Moreover, extending the framework to handle time-series observational data would  
 343 be an interesting direction for future research. Additionally, investigating statistical inference under  
 344 the proposed fusion framework would be valuable.

345 **References**

- 346 Angrist, J. D., Imbens, G. W., and Rubin, D. B. (1996). Identification of causal effects using instru-  
347 mental variables. *Journal of the American Statistical Association*, 91(434):444–455.
- 348 Athey, S. and Imbens, G. (2016). Recursive partitioning for heterogeneous causal effects: Table 1.  
349 *Proceedings of the National Academy of Sciences*, 113:7353–7360.
- 350 Athey, S., Tibshirani, J., and Wager, S. (2019). Generalized random forests. *The Annals of Statistics*,  
351 47(2):1148 – 1178.
- 352 Bareinboim, E. and Pearl, J. (2016). Causal inference and the data-fusion problem. *Proceedings of*  
353 *the National Academy of Sciences*, 113:7345–7352.
- 354 Breiman, L. (2001). Random Forests. *Machine Learning*, 45:5–32.
- 355 Breiman, L., Friedman, J., Olshen, R., and Stone, C. (1984). *Classification And Regression Trees*.  
356 Chapman & Hall/CRC.
- 357 Buchanan, A. L., Hudgens, M. G., Cole, S. R., Mollan, K. R., Sax, P. E., Daar, E. S., Adimora,  
358 A. A., Eron, J. J., and Mugavero, M. J. (2018). Generalizing Evidence from Randomized Trials  
359 Using Inverse Probability of Sampling Weights. *Journal of the Royal Statistical Society Series A:*  
360 *Statistics in Society*, 181(4):1193–1209.
- 361 Colnet, B., Mayer, I., Chen, G., Dieng, A., Li, R., Varoquaux, G., Vert, J.-P., Josse, J., and Yang, S.  
362 (2020). Causal inference methods for combining randomized trials and observational studies: a  
363 review. *arXiv preprint arXiv:2011.08047*.
- 364 Cui, Y., Pu, H., Shi, X., Miao, W., and Tchetgen, E. T. (2023). Semiparametric Proximal Causal  
365 Inference. *Journal of the American Statistical Association*, 0(0):1–12.
- 366 Dahabreh, I. J., Robertson, S. E., Tchetgen, E. J., Stuart, E. A., and Hernán, M. A. (2019). Gen-  
367 eralizing causal inferences from individuals in randomized trials to all trial-eligible individuals.  
368 *Biometrics*, 75(2):685–694.
- 369 Edwards, S., Lilford, R., Braunholtz, D., Jackson, J., Hewison, J., and Thornton, J. (1999). Ethical  
370 issues in the design and conduct of Randomised Controlled Trials. *Health technology assessment*  
371 *(Winchester, England)*, 2:i–vi, 1.
- 372 Efron, B. (1979). Bootstrap Methods: Another Look at the Jackknife. *The Annals of Statistics*,  
373 7(1):1 – 26.
- 374 Efron, B. and Morris, C. (1973). Stein’s estimation rule and its competitors—an empirical bayes  
375 approach. *Journal of the American Statistical Association*, 68(341):117–130.
- 376 Frangakis, C. and Rubin, D. B. (2002). Principal stratification in causal inference. *Biometrics*, 58.
- 377 Friedman, J. H. (2001). Greedy function approximation: A gradient boosting machine. *The Annals*  
378 *of Statistics*, 29(5):1189 – 1232.
- 379 Glass, T. A., Goodman, S. N., Hernán, M. A., and Samet, J. M. (2013). Causal inference in public  
380 health. *Annual review of public health*, 34:61–75.
- 381 Green, E. and Strawderman, W. (1991). A James-Stein type estimator for combining unbiased and  
382 possibly biased estimators. *Journal of The American Statistical Association - J AMER STATIST*  
383 *ASSN*, 86:1001–1006.
- 384 Györfi, L., Köhler, M., Krzyżak, A., and Walk, H. (2002). *A distribution-free theory of nonparamet-*  
385 *ric regression*, volume 1. Springer.
- 386 Hall, P. (1992). *The bootstrap and Edgeworth expansion* . Springer-Verlag New York.
- 387 Hastie, T., Tibshirani, R., and Friedman, J. (2009). *The Elements of Statistical Learning : Data*  
388 *Mining, Inference, and Prediction*. Springer series in statistics. Springer, 2nd edition.

- 389 Imbens, G. W. and Rubin, D. B. (2016). *Causal inference for statistics, social, and biomedical*  
390 *sciences: An introduction*. Taylor & Francis.
- 391 Kallus, N., Puli, A. M., and Shalit, U. (2018). Removing hidden confounding by experimental  
392 grounding. In Bengio, S., Wallach, H., Larochelle, H., Grauman, K., Cesa-Bianchi, N., and  
393 Garnett, R., editors, *Advances in Neural Information Processing Systems*, volume 31. Curran  
394 Associates, Inc.
- 395 Kosorok, M. and Laber, E. (2019). Precision medicine. *Annual Review of Statistics and Its Applica-*  
396 *tion*, 6:263–286.
- 397 Krueger, A. (1999). Experimental Estimates Of Education Production Functions. *The Quarterly*  
398 *Journal of Economics*, 114:497–532.
- 399 Kuroki, M. and Pearl, J. (2014). Measurement bias and effect restoration in causal inference.  
400 *Biometrika*, 101(2):423–437.
- 401 Künzel, S., Sekhon, J., Bickel, P., and Yu, B. (2019). Meta-learners for estimating heterogeneous  
402 treatment effects using machine learning. *Proceedings of the National Academy of Sciences*,  
403 116:4156–4165.
- 404 Miao, W., Geng, Z., and Tchetgen Tchetgen, E. J. (2018). Identifying causal effects with proxy  
405 variables of an unmeasured confounder. *Biometrika*, 105(4):987–993.
- 406 Nie, X. and Wager, S. (2020). Quasi-oracle estimation of heterogeneous treatment effects.  
407 *Biometrika*, 108(2):299–319.
- 408 Powers, S., Qian, J., Jung, K., Schuler, A., Shah, N., Hastie, T., and Tibshirani, R. (2017). Some  
409 methods for heterogeneous treatment effect estimation in high-dimensions. *Statistics in Medicine*,  
410 37.
- 411 Radcliffe, N. J. and Surry, P. D. (2012). Real-world uplift modelling with significance-based uplift  
412 trees.
- 413 Rosenbaum, P. and Rubin, D. (1983). Assessing Sensitivity to an Unobserved Binary Covariate in  
414 an Observational Study with Binary Outcome. *Journal of the Royal Statistical Society. Series B*  
415 *(Methodological)*, 45(2):212–218.
- 416 Rubin, D. (1974). Estimating causal effects of treatments in randomized and nonrandomized studies.  
417 *Journal of Educational Psychology*, 66.
- 418 Scornet, E., Biau, G., and Vert, J.-P. (2015). Consistency of random forests. *The Annals of Statistics*,  
419 43(4):1716 – 1741.
- 420 Shi, X., Miao, W., Nelson, J., and Tchetgen, E. (2020). Multiply robust causal inference with  
421 double-negative control adjustment for categorical unmeasured confounding. *Journal of the Royal*  
422 *Statistical Society: Series B (Statistical Methodology)*, 82.
- 423 Shi, X., Pan, Z., and Miao, W. (2022). Data integration in causal inference. *WIREs Computational*  
424 *Statistics*, 15(1).
- 425 Taddy, M., Gardner, M., Chen, L., and Draper, D. (2016). A nonparametric bayesian analysis  
426 of heterogenous treatment effects in digital experimentation. *Journal of Business & Economic*  
427 *Statistics*, 34.
- 428 Tang, C., Wang, H., Li, X., Cui, Q., Zhang, Y.-L., Zhu, F., Li, L., Zhou, J., and Jiang, L. (2022).  
429 Debiased causal tree: Heterogeneous treatment effects estimation with unmeasured confounding.  
430 In Koyejo, S., Mohamed, S., Agarwal, A., Belgrave, D., Cho, K., and Oh, A., editors, *Advances*  
431 *in Neural Information Processing Systems*, volume 35, pages 5628–5640. Curran Associates, Inc.
- 432 Turney, K. and Wildeman, C. (2015). Detrimental for some? heterogeneous effects of maternal  
433 incarceration on child wellbeing. *Criminology & Public Policy*, 14.
- 434 Wager, S. and Athey, S. (2018). Estimation and inference of heterogeneous treatment effects using  
435 random forests. *Journal of the American Statistical Association*, 113(523):1228–1242.

- 436 Wu, L. and Yang, S. (2022). Transfer learning of individualized treatment rules from experimental  
437 to real-world data. *Journal of Computational and Graphical Statistics*, 0(0):1–10.
- 438 Yang, S., Zeng, D., and Wang, X. (2020). Improved inference for heterogeneous treatment effects  
439 using real-world data subject to hidden confounding. *arXiv preprint arXiv:2007.12922*.
- 440 Zhang, B. and Tchetgen Tchetgen, E. J. (2022). A Semi-Parametric Approach to Model-Based  
441 Sensitivity Analysis in Observational Studies. *Journal of the Royal Statistical Society Series A:  
442 Statistics in Society*, 185:S668–S691.
- 443 Zhang, H., Zimmerman, J., Nettleton, D., and Nordman, D. J. (2020). Random Forest Prediction  
444 Intervals. *The American Statistician*, 74(4):392–406.